

PAPER

## Dexamethasone loaded Laponite<sup>®</sup>/porous calcium phosphate cement for treatment of bone defects

To cite this article: Mehran Roozbahani and Mahshid Kharaziha 2019 *Biomed. Mater.* **14** 055008

View the [article online](#) for updates and enhancements.



**IOP | ebooks<sup>™</sup>**

Bringing you innovative digital publishing with leading voices to create your essential collection of books in STEM research.

Start exploring the collection - download the first chapter of every title for free.

# Biomedical Materials



## PAPER

# Dexamethasone loaded Laponite<sup>®</sup> / porous calcium phosphate cement for treatment of bone defects

RECEIVED  
11 January 2019

REVISED  
21 June 2019

ACCEPTED FOR PUBLICATION  
18 July 2019

PUBLISHED  
2 August 2019

Mehran Roozbahani and Mahshid Kharaziha<sup>1</sup>

Department of Materials Engineering, Isfahan University of Technology, Isfahan 84156-83111, Iran

<sup>1</sup> Author to whom any correspondence should be addressed.

E-mail: [kharaziha@cc.iut.ac.ir](mailto:kharaziha@cc.iut.ac.ir)

**Keywords:** calcium phosphate based cement, Laponite nanoplates, porous cement, mechanical properties

## Abstract

In this research, nanocomposite porous calcium phosphate cements (CPCs) consisting of dexamethasone (DEX) loaded Laponite<sup>®</sup> nanoplates (LAP) (DEX-LAP) were fabricated and the effects of sodium bicarbonate (NaHCO<sub>3</sub>) as the foaming agent on the physical, mechanical, and biological characteristics of DEX-LAP loaded CPCs were investigated. Our findings showed that DEX-LAP encapsulation significantly reduced the final setting time (1.5 times) of CPCs and accelerated the total transformation of tricalcium phosphate to hydroxyapatite. Moreover, DEX-LAP nanoplates meaningfully enhanced the compressive strength (4 fold) and compressive modulus (4 fold) of cement. Additionally, incorporation of 6% foaming agent noticeably reduced setting time of cement to less than 10 min due to the enhanced surface area in contact with cement paste. Encapsulation of DEX within the LAP nanoplates and consequently loading of DEX-LAP nanoplates in the CPCs resulted in the significantly reduced burst release of DEX. Finally, the results also illustrated that the presence of interconnected micropores and DEX-LAP nanoplates in the CPC improved MG63 cell proliferation. These findings suggest that the porous DEX-LAP/CPC can potentially be developed as bone grafts for bone defects.

## 1. Introduction

By increasing the number of musculoskeletal injuries including bone defects and development of minimally invasive surgeries, researches have been focused on the biomaterials with the ability to promote bone regeneration (Ginebra and Montufar 2014). Thanks to the similarity with the mineral section of bone, biocompatibility and, osteoconductivity, calcium phosphate-based constituents are extensively applied for filling bone defects in two main forms of ceramics and cements (Verron *et al* 2012). The advantages of calcium phosphate cements (CPCs) to ceramics consisting of self-setting, injectability, plasticity, minimally invasive injection and compatibility with complicated defects result in the wide development of CPCs for filling bone defects. In addition, thanks to natural capacity to adsorb bioactive agents and low setting temperature, CPCs have been applied as drug carriers for treatment of skeletal system diseases like osteoarthritis, osteoporosis and rheumatoid arthritis (Ginebra *et al* 2012). For instance, Roy *et al* (2016)

developed a resorbable composite of CPC-poly (lactic acid-co-glycolic acid) (PLGA) microspheres in which vancomycin drug was encapsulated into PLGA microspheres. Results revealed the efficient long-term controlled release of vancomycin more than 10 weeks from CPC (Roy *et al* 2016). Among the various types of drugs and biomolecules, dexamethasone (DEX) has been widely applied for bone tissue engineering. DEX is an anti-inflammatory and immunosuppressant drug which has been widely applied to treat the inflammatory diseases. Moreover, DEX molecule plays important roles on the regulation of genes and cellular reactions responsible for the growth and division of cells. In a research, Kharaziha *et al* (2015) found the importance of DEX to stimulate the osteoblast differentiation of stem cells and, consequently, facilitate tissue remodeling. In another research, DEX was directly loaded in a free-pore cement to evaluate the release of drug from CPC. The findings revealed that the DEX release from the cement was sustained and no burst release was observed (Forouzandeh *et al* 2014).

In spite of suitable properties of these types of cement, their main drawback is the lack of microporosity, preventing from cell infiltration, forming vessel inside pores and connection with the host tissue. To overcome these issues, self-setting, injectable and, porous CPCs have been developed using foaming agents such as albumin (Ginebra and VSD 2007), soybean (Perut *et al* 2011), mannitol (Tang *et al* 2012), sucrose (Takagi and Chow 2002) and sodium bicarbonate ( $\text{NaHCO}_3$ ). Introduction of macro-pores into CPCs enhances injectability and promotes the interconnection of cement with the host tissue (DelReal *et al* 2002, Ginebra and Montufar 2014). In addition, micropores (pores larger than  $100\ \mu\text{m}$ ) are introduced into CPCs in order to facilitate bone ingrowth, implant fixation, cell colonization and, angiogenesis. Among them, sodium bicarbonate ( $\text{NaHCO}_3$ ) as an inorganic foaming agent could enhance the efficiency of the foaming process and increase the quality of the foamed cement. Moreover,  $\text{NaHCO}_3$  has been widely used to increase both passive and active resorption of cement, former refers to the formation of carbonateapatite in the presence of  $\text{NaHCO}_3$ , and latter is the creation of macropores during cement formation process due to  $\text{CO}_2$  bubble formation (DelReal *et al* 2002). In contrary, most of foaming agents such as Mannitol could form micro-pores in the cements only due to gradual degradation after complete cementation (Tang *et al* 2012). Moreover, Some of them such as sucrose could not totally dissolve upon formation of cement and remain unreacted in the cement (Takagi and Chow 2002). DelReal *et al* (2002) used  $\text{NaHCO}_3$  as a foaming agent. In this method,  $\text{CO}_2$  bubbles formed as a result of a mixture of powder and acidic liquid phases bring about to formation of micropores (pores of foam were about  $100\ \mu\text{m}$ ).

Another restriction of CPCs is their weak mechanical properties, making them unsuitable for load-bearing situations (Ginebra *et al* 2012). The ultimate mechanical strength of the CPC was modulated based on the degree of cement transformation, the kind of setting result, the porosity of the cement and the crystallite size of the filler particles (Roozbahani *et al* 2017a). For this reason, many studies have been carried out for designing and fabrication of various types of composite CPC with great mechanical properties (Cama and Barberis 2009, Mohammadi *et al* 2014, Tancret and Liu 2014, Gbureck *et al* 2015). A favorable strategy is reinforcing with nanoparticles (Mohammadi *et al* 2014), polymeric (Xu *et al* 2008) and, metallic (Krüger *et al* 2013) fibers, bioresorbable fibers (Xu and Quinn 2002) and/or whiskers of calcium minerals (Müller *et al* 2007, Zhao *et al* 2012). For instance, Mohammadi *et al* (2014) investigated the effects of SiC,  $\text{TiO}_2$  and  $\text{SiO}_2$  nanoparticle addition on the mechanical properties of porous CPCs. Results illustrated that while the compressive strength of the CPC was increased 10 and 15 times in the presence 5 and 10 wt% of  $\text{TiO}_2$  nanoparticles, respectively, no

considerable change was detected in the presence of SiC nanoparticles due to lack of effective bonds at the SiC nanoparticles-CPC interfaces. Also, addition of  $\text{SiO}_2$  nanoparticles in the CPCs indicated maximum the compressive strength values of the CPCs. It could be suggested that improved mechanical strength of  $\text{TiO}_2$  and  $\text{SiO}_2$ -added CPCs was due to the fact that these nanoparticles filled pores of CPCs and created a compacted microstructure (Mohammadi *et al* 2014).

Lately, the synthetic nanoclays of Laponite<sup>®</sup> ( $\text{Na}_{0.7}[(\text{Mg}_{5.5}\text{Li}_{0.3})\text{Si}_8\text{O}_{20}(\text{OH})_4]_{0.7}$ , LAP) has been presented as a biocompatible disk-shaped silicate belonging to the family of phyllosilicates (Ruzicka and Zaccarelli 2011, Wang *et al* 2014). Thanks to the exceptional characteristics consisting of swelling in water, ability to cation exchange, high specific area, pH-dependent edge charge and suitable interface with organic and inorganic constituents, LAP has been widely applied for bone tissue engineering and drug delivery systems (Gaharwar *et al* 2019). In aqueous conditions, LAP nanoplates degrade into bioactive products stimulating bone formation and growth in different stages (Hoppe *et al* 2011, Liu *et al* 2015). Moreover, results confirmed that LAP nanoplates in a colloid gel shape are able to enrich stem cell differentiation (Ghadiri *et al* 2015). Gaharwar *et al* (2013) proved that LAP nanoplates encouraged the osteogenic differentiation of mesenchymal stem cells and tightly interacted with the stem cells (Gaharwar *et al* 2013, Carrow *et al* 2018). They also developed LAP-poly (ethylene oxide) (PEO) nanocomposite and found the promotion of osteogenic differentiation of stem cells in the presence of LAP nanoplates in the nanocomposites (Gaharwar *et al* 2012). In addition to these properties, as aforementioned, due to the high specific surface area and gel-forming ability, LAP nanoplates have been widely employed as carriers for drugs and macromolecules such as donepezil (Park *et al* 2008), tetracycline (Ghadiri *et al* 2013), DEX (Fraile *et al* 2016) and doxorubicin (Wang *et al* 2013). For instance, Ghadiri *et al* (2013) used LAP nanoplates as a drug carrier for *in situ* delivery of tetracycline and demonstrated that controlled release of tetracycline from LAP nanoplates took place upon a 72 h period. Recently, we encapsulated DEX into LAP nanoplates and confirmed LAP nanoplates could be a promising candidate for controlled release of anionic DEX in the controlled manner depending on the pH environment. Moreover, the merits of LD-NPs such as great cytocompatibility, excellent physiological stability and sustained pH-responsive release properties, make them a promising platform for the delivery of other therapeutic agents beyond DEX (Roozbahani *et al* 2017b).

In this study, we aim to develop innovative nanocomposite porous DEX loaded-Laponite<sup>®</sup> (DEX-LAP)/calcium phosphate bone cement and investigate the role of DEX-LAP nanoplates on the physical and mechanical characteristics of bone cement. Furthermore, the effect of introducing micropores on the

physical and mechanical properties of DEX-LAP/CPCs was investigated. Moreover, the release kinetics of DEX from CPCs was also evaluated on the cell behavior. It is hypothesized that incorporation of DEX loaded LAP nanoplates as well as microporous structure of CPCs could promote bone regeneration.

## 2. Experimental section

### 2.1. Materials

Calcium nitrate ( $\text{Ca}(\text{NO}_3)_2$ ) and phosphorus pentoxide ( $\text{P}_2\text{O}_5$ ), sodium dihydrogen phosphate ( $\text{NaH}_2\text{PO}_4$ ), amorphous silica ( $\text{SiO}_2$ ), sodium bicarbonate ( $\text{NaHCO}_3$ ) and disodium hydrogen phosphate ( $\text{Na}_2\text{HPO}_4$ ) were purchased from Merck Co. DEX was obtained from Sigma Aldrich (95% purity). Synthetic silicate nanoplatelets (Laponite<sup>®</sup> RDS) was obtained from Rockwood, UK.

### 2.2. Preparation of DEX-LAP nanoplates

DEX-LAP nanoplates were prepared according to the optimized procedure presented in our previous research (Roozbahani *et al* 2017a, 2017b). Briefly, 10 mg ml<sup>-1</sup> LAP nanoplates suspension in deionized water was prepared and pH of the suspension was set to 3 using 0.1 M HCl. The suspension was sonicated for 15 min to provide homogenous suspension. After addition of DEX to LAP suspension (at a constant content of 2 mg ml<sup>-1</sup>), it was stirred magnetically at room temperature for 24 h to expand the distance between LAP layers and form DEX-LAP nanoplates. As prepared DEX-LAP suspension was centrifuged (6000 rpm, 20 min) to extract DEX-LAP nanoplates. Consequently, after three-times rinsing with DI water, to remove non-immobilized DEX, DEX-LAP nanoplates were dried in air.

### 2.3. Fabrication of porous nanocomposite DEX-LAP/calcium phosphate bone cement

The calcium phosphate bone cement consisted of two components of liquid and powder phases. The powder phase of CPCs applied in this research consisted of 98 wt%  $\alpha$ -tricalcium phosphate ( $\alpha$ -TCP) and 2 wt% hydroxyapatite (HA) nanoparticles. These two components were synthesized using sol-gel process according to our previous report (Roozbahani *et al* 2017a). The fabrication process of porous nanocomposite calcium phosphate bone cement is schematically illustrated in figure 1. Initially, a mixture of 98 wt%  $\alpha$ -TCP, 2 wt% HA and 2 wt% DEX-LAP nanoplates was prepared using ball milling at 250 rpm for 1 h. Separately, the liquid phase consisting of 8 wt%  $\text{Na}_2\text{HPO}_4$ , 8 wt%  $\text{NaH}_2\text{PO}_4$  and  $\text{NaHCO}_3$ , as the foaming agent, was prepared. Consequently, powder component and liquid phase were combined in a constant powder to liquid ratio of 1. Consequently, the made paste was dispensed into a cylindrical mold (diameter = 10 mm, height = 15 mm) and kept at 37 °C in 100% relative humidity for specific time point

(1, 3 and 5 d). To investigate the role of foaming agents on the characteristics of CPCs, two different amounts of  $\text{NaHCO}_3$  (3 and 6 wt%) were added to the liquid phase mixture. According to the amounts of foaming agent contents, the samples were labeled, according to table 1. CPC without DEX-LAP nanoplates was also similarly reported as the control (CTL).

### 2.4. Characterization of porous nanocomposite DEX-LAP/calcium phosphate bone cement

The chemical composition of calcium phosphate bone cement, consisting of  $\alpha$ -TCP, HA, and DEX-LAP nanoplates and cement samples was assessed by x-ray diffraction (XRD, Philips X'pert, Cu K $\alpha$  radiation). Furthermore, Scherer equation was applied to estimate the crystallite size of HA component in the cements. The morphology of various types of nanocomposite cement was evaluated by field emission scanning electron microscope (FE-SEM, MIRA3 TESCAN).

The injectability and setting time of the porous nanocomposite cements in the cylindrical molds with a dimension of 10 mm (diameter) and 15 mm (height) were also investigated. In this regard, the injectability of CPCs was examined by using a syringe with an aperture diameter of 2 mm. The CPC pastes were entirely extruded from the syringe under hand pressure. After mixing for 150 s, the CPC injectability was estimated by the fraction of the paste weights extruded from the syringe and the total paste in the syringe (Maenz *et al* 2014). Setting time of the porous nanocomposite CPCs was measured by using Vicat needle based on ISO 9917 standard. According to this method, the final setting time took place when the nozzle did not sink visibly into the paste (ASTM, C. 2003). Therefore, after mixing the liquid and powder phases, the CPCs were placed in 0.9% saline at 37 °C in 100% humidity and final setting time was estimated using Vicat needle (Model 1802, Germany) (Kim and Jeon 2012). The plasticity of the cement was also determined by using star-shaped molds. In this regard, the cement paste was poured into the star molds by using a syringe and was placed at the aqueous medium (0.9% saline) with relatively 100% humidity at 37 °C.

Mechanical characteristics of the cement were investigated using the Instron universal Machine. The cement pastes poured in cylindrical molds were retained in a medium with 100% humidity for the specific time points (1, 3 and 5 d). Finally, after drying, the cements were compacted at a speed of 0.5 mm min<sup>-1</sup> (ASTM C1424-15) (Kim and Jeon 2012). To estimate the percentage of apparent porosity of the cements, Archimedes' principle was employed according to equation (1):

$$\text{Apparent porosity} = \frac{W_{\text{wet}} - W_{\text{d}}}{W_{\text{wet}} - W_{\text{su}}} \times 100. \quad (1)$$

In which  $W_{\text{wet}}$  stands for wet weight,  $W_{\text{d}}$  and  $W_{\text{su}}$  state dry and immersion weight, respectively.

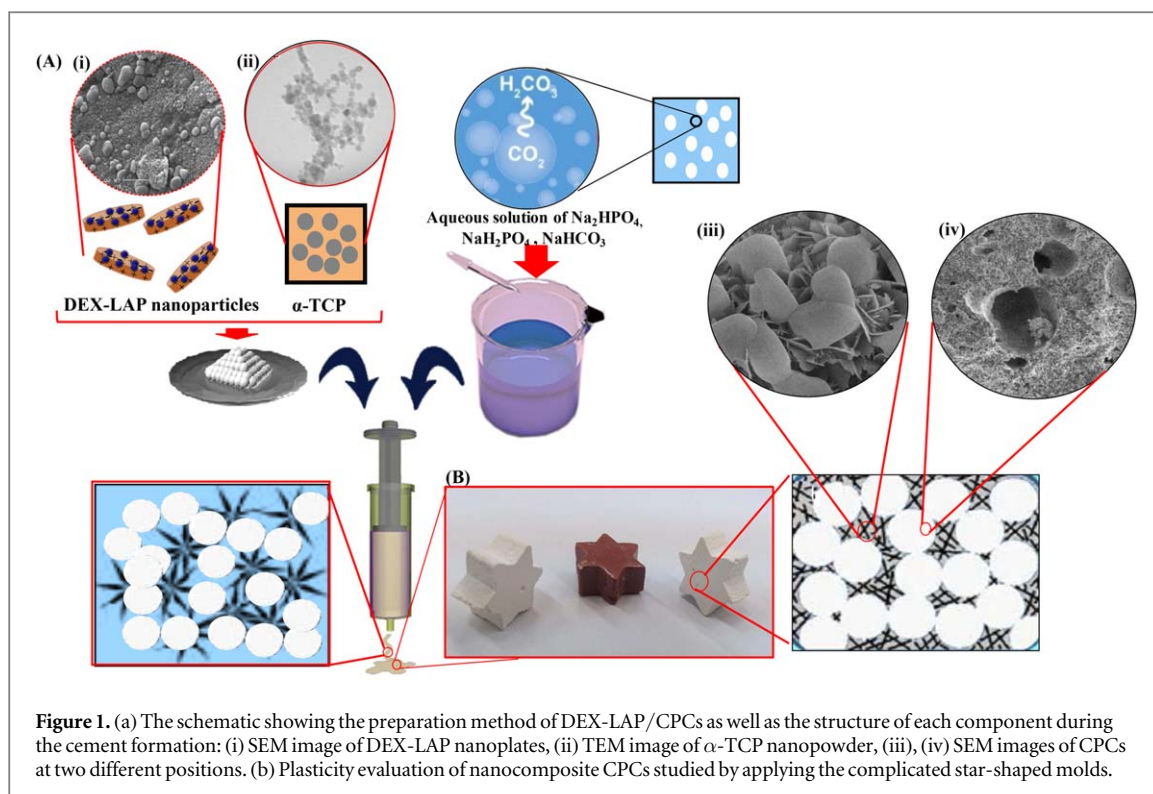


**Figure 1.** (a) The schematic showing the preparation method of DEX-LAP/CPCs as well as the structure of each component during the cement formation: (i) SEM image of DEX-LAP nanoplates, (ii) TEM image of  $\alpha$ -TCP nanopowder, (iii), (iv) SEM images of CPCs at two different positions. (b) Plasticity evaluation of nanocomposite CPCs studied by applying the complicated star-shaped molds.

**Table 1.** Composition of prepared porous samples and measurements of final setting time (min) and injectability.

Sample		CPC(CTL)	CPC-2	CPC-2-3	CPC-2-6
Liquid phase (%)	$\text{Na}_2\text{HPO}_4$	50	50	50	50
	$\text{NaH}_2\text{PO}_4$	50	50	50	50
Foaming agent ( $\text{NaHCO}_3$ ) (gr)		0	0	3	6
	DEX-LAP nanoplates	0	2	2	2
Final setting time (min)		$17.6 \pm 1$	$12.3 \pm 1$	$9.7 \pm 1$	$9.6 \pm 1$
Injectability (%)		90	92	90	92

## 2.5. Drug release study

To study the DEX release from CPCs, the samples with a dimension of  $10 \times 5 \text{ mm}^2$  ( $n = 3$ ) were placed into 12 ml PBS and consequently were incubated at  $37^\circ\text{C}$  for various pre-determined intervals (3, 17, 40, and 70 h). It is worth mentioning that PBS solution was refreshed at each pre-determined interval time. Consequently, the amount of released DEX ( $\text{mg ml}^{-1}$ ) in each interval was estimated by using UV-vis spectrophotometer at the highest wavelength of DEX absorbance (242 nm). It needs to mention that, the amounts of DEX was approximately calculated by using a calibration curve of DEX obtained in a similar solution.

## 2.6. Cell culture

In order to evaluate *in vitro* cytocompatibility of porous cement, cellular experiments were performed. Accordingly, osteoblast-like cells (MG63 cell line) was purchased from the National Cell Bank of Iran. Firstly, the set cements were sterilized in 70% ethanol for 30 min and, subsequently, were exposed for 20 min

under ultraviolet light. In following, after incubation in a culture medium consisting of Dulbecco's Modified Eagle Medium (Gibco) enriched with 10% fetal bovine serum (Gibco) and 1% penicillin-streptomycin (Gibco), overnight, MG63 cells were seeded on the samples at a density of  $1 \times 10^4$  cells per well and incubated at  $37^\circ\text{C}$  and 5%  $\text{CO}_2$  upon 7 d. Upon incubation, the culture medium of each plate was taken out and the fresh culture medium was replaced, every 3 d.

MG63 cell proliferation on the samples was assessed using MTT (3-(4,5-Dimethylthiazol-2-Yl)-2,5-Diphenyltetrazolium Bromide) assay based on the manufacturer's instruction (Sigma). Firstly, after removing the culture medium from each sample, MTT solution ( $0.5 \text{ mg ml}^{-1}$  reagent in culture medium) was added to them, followed by 4 h incubation at  $37^\circ\text{C}$  and 5%  $\text{CO}_2$ . Subsequently,  $300 \mu\text{l}$  DMSO (Sigma) was added to each well and after 30 min incubating at room temperature, the absorbance of DMSO was determined at 570 nm by using Microplate Reader

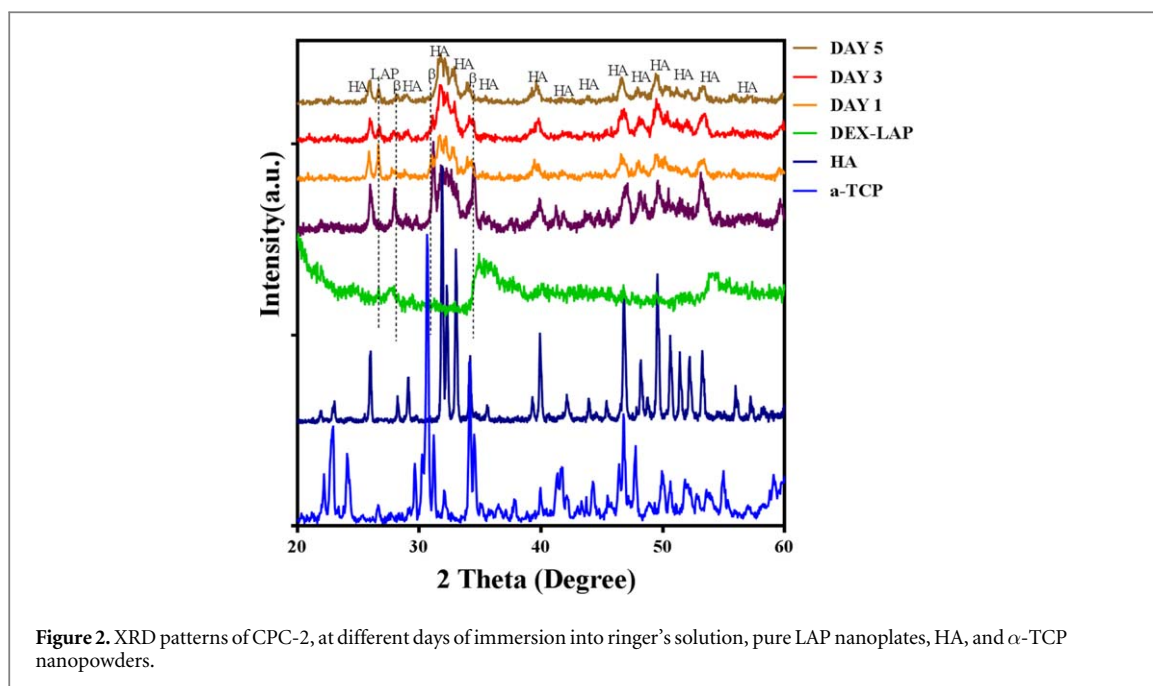


**Figure 2.** XRD patterns of CPC-2, at different days of immersion into ringer's solution, pure LAP nanoplates, HA, and  $\alpha$ -TCP nanopowders.

(Bio Rad, Model 680 instruments). All the experiments were carried out in a triplicate and consequently the optical density of the each well in a plate was reported and two control samples (TCP) were labeled for comparison (Roozbahani *et al* 2017a).

### 2.7. Statistical analysis

Statistical analyses were done via one-way ANOVA ( $n \geq 3$ ). Moreover, to investigate a statistical meaningful difference between groups, Tukey's *post-hoc* test using GraphPad Prism Software (V.6) was applied to be significant.

## 3. Results and discussion

### 3.1. Characterization of porous DEX-LAP/CPC

Porous DEX-LAP/CPC was prepared by a mixture of powder precursors and DEX-LAP nanoplates, according to figure 1. At first, the role of DEX-LAP nanoplates on the characteristics of the CPC was evaluated. Figure 2 shows XRD patterns of pure LAP, CPC (CTL), and CPC-2 after immersion in normal saline for pre-determined intervals (day 1 (DAY 1), 3 (DAY 3), and 5 (DAY 5)). XRD patterns of HA and  $\alpha$ -TCP were presented as the control. XRD patterns of all pure CPC (CTL) consisted of the characteristic peaks of  $\beta$ -TCP at  $2\theta = 28^\circ, 31^\circ$  and  $34^\circ$ , according to the  $\beta$ -TCP standard card (00-009-0169 (ICSD code)). Moreover, the rest of peaks appeared at  $2\theta = 22^\circ, 26^\circ, 32^\circ, 34^\circ, 40^\circ, 47^\circ, 50^\circ$  and  $53^\circ$  were related to the Miller indices of (111), (002), (112), (202), (221), (222), (321), and (004) of HA, respectively, based on the standard card of CDHA (01-086-1199 (ICSD code)). Our results demonstrated that  $\alpha$ -TCP was totally transformed to CDHA and  $\beta$ -TCP phases. However, unlike CPC (CTL), complete conversion of  $\alpha$ -TCP into CDHA

took place after only one day immersing of CPC-2 (DAY 1) in normal saline confirming the acceleration of conversion in the presence of DEX-LAP. In addition, an extra peak at  $2\theta = 26^\circ$  related to DEX-LAP nanoparticles could be detected at XRD patterns of CPC-2 approving the incidence of LAP nanoparticle in the bone cement. Increasing the immersing time did not change the chemical composition of the cement. Similarly, Roy *et al* (2016) incorporated resorbable PLGA microspheres into CPC in order to create micropores and evaluated the effect of PLGA microspheres on conversion of  $\alpha$ -TCP to CDHA. The results demonstrated that transformation of  $\alpha$ -TCP into CDHA did not even take place after 30 d at free-PLGA CPC sample. In contrast, after incorporation of PLGA,  $\alpha$ -TCP phase was never observed in the cement until 30 d after immersing in PBS. On the other hand, according to Sheerer equation, the crystallite size of HA in CPC (CTL) and CPC-2 after a day of immersion (DAY 1) was 48 nm and 31 nm, respectively, proving the finer crystallite size of HA in the presence of DEX-LAP. In other word, DEX-LAP nanoplates provided more nucleation sites, while restricting the extreme growth of calcium phosphate crystals. In addition to reduced crystallite size of HA nucleation, results showed that incorporation of DEX-LAP modulated the injectability and setting time of the CPCs.

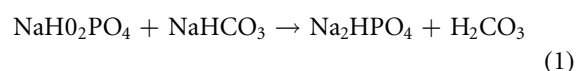
Injectability has been considered as a critical factor in order to use in minimally invasive methods like filling damaged bones caused by osteoporosis and *in situ* fracture fixation. Based on table 1, CPC-2 revealed an injectability value of around 92% that could be reflected as high injectability. Based on previous researches, incorporation of nanoparticles (Roozbahani *et al* 2017b), reduction of reactant particle size (Ginebra *et al* 2004), and formation of hydrogel (Liu *et al* 2014) could lead to the improvement of rheological

properties (injectability, viscosity, and cohesion) of cement paste, while preventing from the separation of powder and liquid phases during injection. Therefore, dispersion of DEX-LAP nanoplates into CPC as a gelling agent resulted in promoted rheological properties such as viscosity and cohesion followed by improvement in injectability of nanocomposite cement. In a similar study, hydroxypropyl methylcellulose was employed as a gelling agent into the structure of CPCs to improve injectability of paste. Results showed the enhanced injectability from 60% to over 90% followed by considerably reduced surgical operation time, minimizing side effects caused by long surgical operation time and eventually cost-effectiveness (Xu *et al* 2008). In another research, in order to enhance rheological properties, Xue *et al* (2012) incorporated PLGA microspheres into CPC and showed that injectability of cement pastes improved from 40.1% to 67.6%. Moreover, the plasticity of the nanocomposite CPCs was assessed by the employment of a complicated mold with star-shape. According to figure 1, the prepared paste was able to penetrate into mold even in sharp edges to achieve the perfect structure of star-shaped CPC. Moreover, results showed that incorporation of LAP-DEX within the CPCs resulted in the reduced setting time of cement from  $17.7 \pm 1$  min to  $12.3 \pm 1$  min. It might be due to the improved water capability, and gel-forming ability via incorporation of DEX-LAP nanoplates. Similarly, Mohammadi *et al* (2014) examined the effect of ceramic nanoparticle incorporation on the setting time of CPC. Their results illustrated the upward trend of initial setting time in the presence of 10 wt% nano-TiO<sub>2</sub> from 12 to 15 min, while incorporation of 10 wt% of SiC and silica brought about to increase 2.3 times and reduce 2 times, respectively. In another study, Shahrezaei *et al* (2014) evaluated the effect of particle size of main precursor on setting time of apatite cement. The results demonstrated a lower initial and final setting time from 20 min to 15 min and from 32 min to 25 min, respectively.

FE-SEM technique was employed to evaluate the morphology of CPC (CTL), and CPC-2 samples, according to figure 3(a), CTL sample consisted of plate-like particles which could be attributed to HA crystals (Ginebra *et al* 2006). After uniform dispersion of DEX-LAP nanoplates (CPC-2) within the CPC (figure 3(b)), these particles became smaller and narrower. Accordingly, while particle size of HA in CPC (CTL) was  $2.8 \pm 1.1$   $\mu\text{m}$ , in the presence of 2 wt% DEX-LAP nanoplates, it was turned to  $37.6 \pm 12.2$  nm. DEX-LAP nanoplates acted as nucleating agents for HA crystals which resulted in enhanced nucleating situations. Consequently, these agents prohibited from HA growth and made homogenous deposition of HA crystals. Similarly, Liu *et al* (2016) developed composite cement containing wollastonite (WS) and investigated the effect of WS on the microstructure of CPC. The results showed that after 1 week of soaking in PBS, some tiny

flake-shaped apatite started forming on the surface of CPC/WS. Moreover, they found that flake-shaped apatite crystals became smaller and much denser than in the CPC/WS compared to pure CPC.

After incorporation of foaming agent (sodium bicarbonate), uniform micropores with the dominant size between 50 and 100  $\mu\text{m}$  and with isodiametric shapes were formed in the bone cement (figures 4(a) and (b)). However, the average size of these pores was depended on the proportion of sodium bicarbonate. Frequency distribution of micro-pore size at both samples are presented in figures 4(a) and (b). Results showed that, at CPC-2-3 sample, approximately 50% of pore size was in the range of 50–100  $\mu\text{m}$ . At this sample, the apparent porosity, measured by Archimedes method, was estimated about  $45 \pm 4\%$ . However, as the foaming agent concentration increased from 3% to 6%, the apparent porosity raised to  $58 \pm 6\%$  and frequency distribution showed a wide range of different pore sizes from less than 20  $\mu\text{m}$  to more than 150  $\mu\text{m}$ . Between these ranges, more than 20% of the pore sizes were over 150  $\mu\text{m}$ . This pore size is necessary for cell adhesion and ingrowth (Montufar *et al* 2010). The pore formation could be due to the reaction between NaHCO<sub>3</sub> and NaH<sub>2</sub>PO<sub>4</sub>, as well as the formation of acidic medium to accelerate decomposition of H<sub>2</sub>CO<sub>3</sub> (reaction 1), followed by formation of CO<sub>2</sub> bubbles in the whole structure of cement (reaction 2). Incorporation of acidic liquid phase not only favors fast hardening of cement paste, but it also provides an acidic medium to fast decomposition of NaHCO<sub>3</sub> into H<sub>2</sub>CO<sub>3</sub>



Moreover, according to figure 4(c), the average pore size of the cements significantly increased from  $98 \pm 22$   $\mu\text{m}$  to more than  $148 \pm 18$   $\mu\text{m}$ , when the foaming agent concentration enhanced from 3% to 6% ( $P < 0.05$ ). DelReal *et al* (2002) similarly applied NaHCO<sub>3</sub> as the foaming agent to introduce micropores into CPCs via formation of CO<sub>2</sub> bubbles through decomposition of H<sub>2</sub>CO<sub>3</sub>. They showed the formation of micropores with the average size of 100  $\mu\text{m}$  and total porosity of 50%. Moreover, according to table 1, the presence of NaHCO<sub>3</sub> as the foaming agent in the NaH<sub>2</sub>PO<sub>4</sub> aqueous solution considerably reduced setting time of CPC paste. It could be due to the fact that pores created in the presence of foaming agent and formation of CO<sub>2</sub> bubbles which enhanced the surface area in contact with cement paste followed by accelerating nucleation and crystallization of HA and then fast setting. Generally, CPC pastes form by the development of a solid network which could be affected by the hydrolysis degree of precursors. The prerequisite energy for the construction of this solid complex is offered by surface energy created from both liquid and powder components. Consequently, a

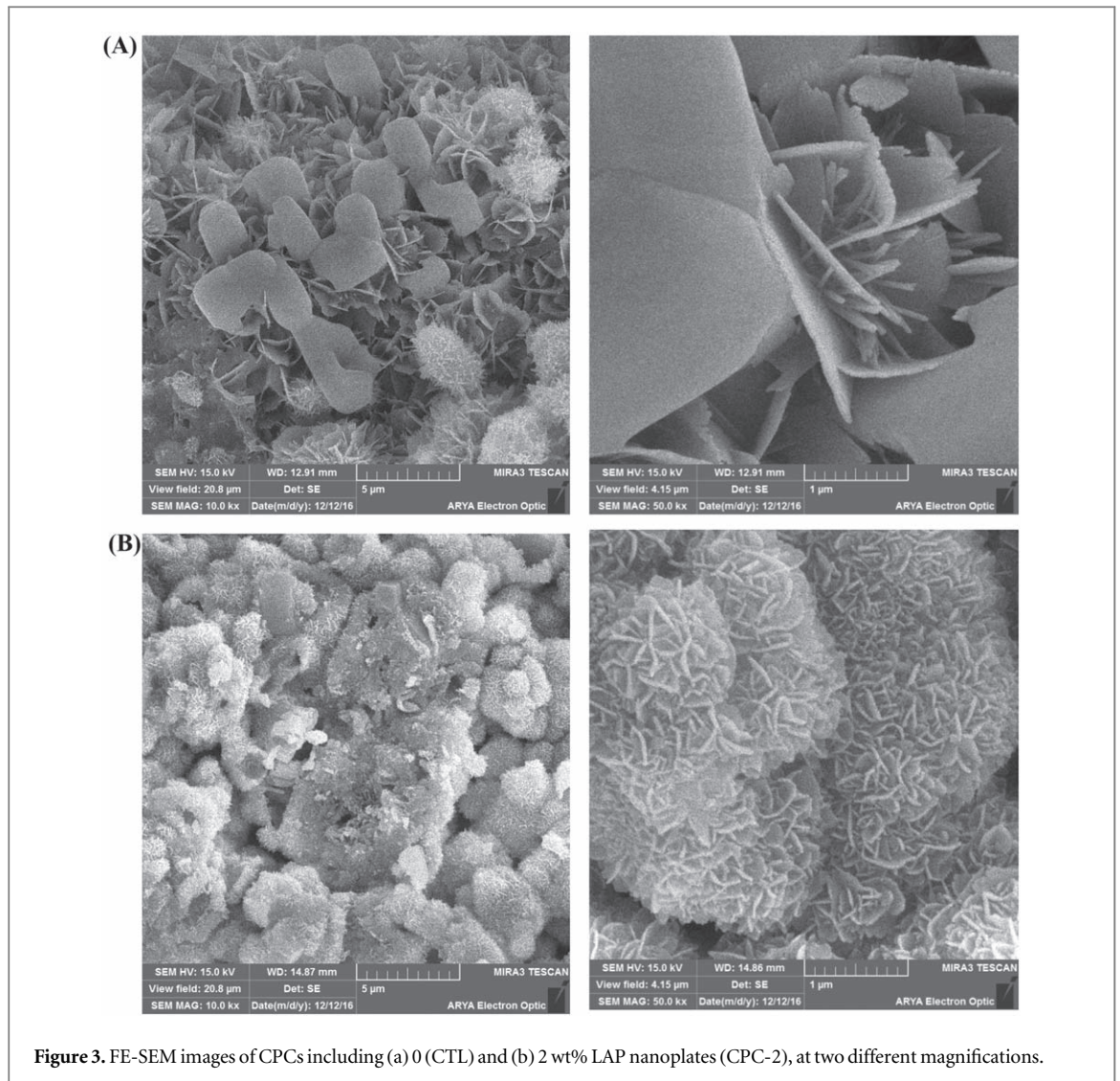
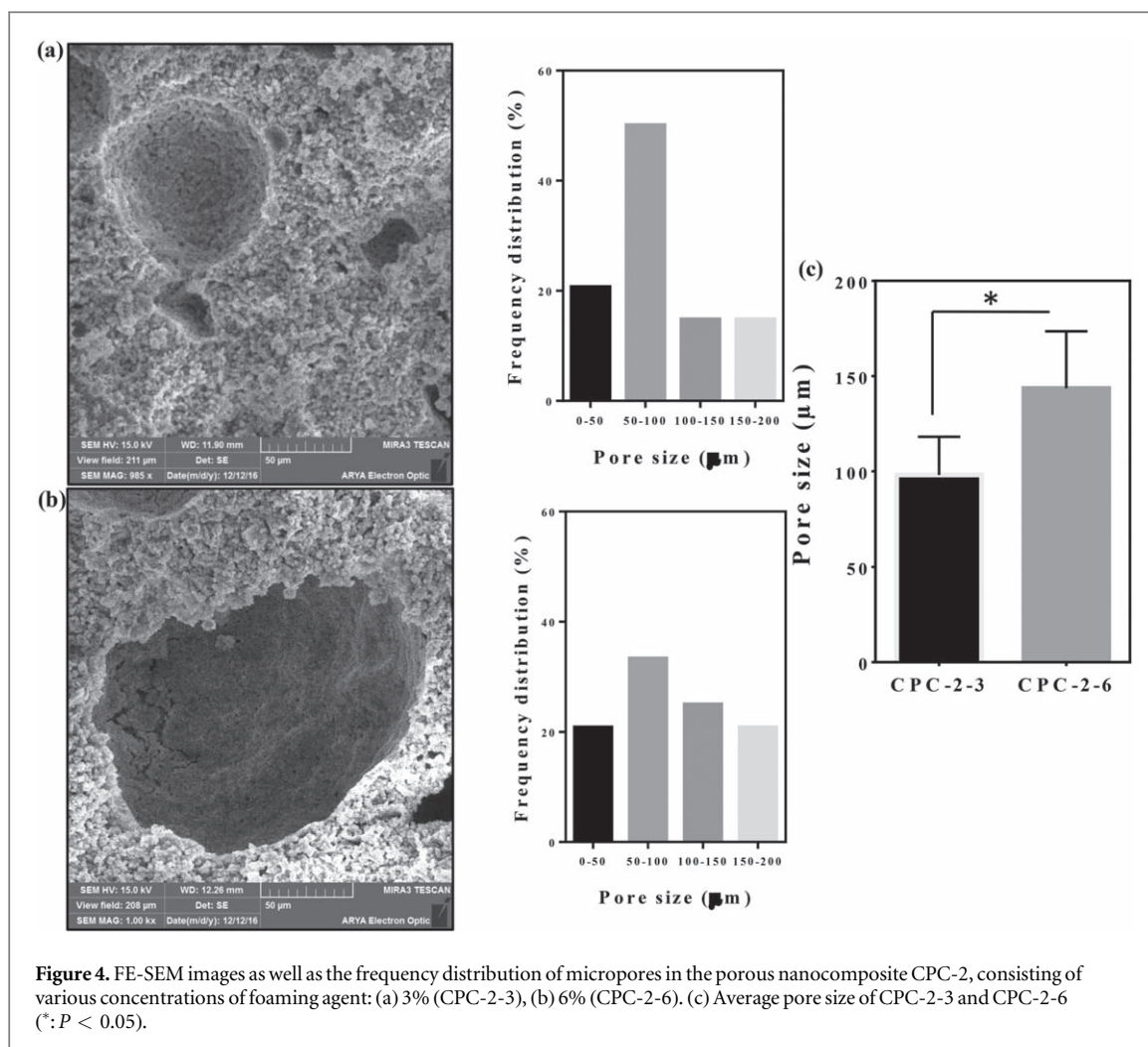


**Figure 3.** FE-SEM images of CPCs including (a) 0 (CTL) and (b) 2 wt% LAP nanoplates (CPC-2), at two different magnifications.

superior hydrolysis reaction rate resulted in the reduced setting time. Our results revealed that the presence of DEX-LAP nanoplates and foaming agent, as well as nanometric reactants could respectively affect the rheological properties, fast setting and an improvement in conversation rate of precursors leading to a significant reduction in the final setting time and great initial setting rate of the porous cement.

Basically, the major issue associated with CPCs is their weak mechanical properties making them unsuitable for load-bearing applications (DelReal *et al* 2002). Stress–strain diagrams of all samples are presented in figure 5(a). A similar stress–strain behavior was observed in all samples. Due to the presence of micro/nanopores in calcium phosphate, a brittle fracture behavior could be recognized. However, according to figures 5(b) and (c), DEX-LAP incorporation resulted in significant improvement in the compressive strength and modulus of the CPCs, after 5 days of immersion, respectively. Results revealed that the compressive strength and modulus of the CTL ( $1.05 \pm 0.21$  MPa and  $0.54 \pm 0.14$  GPa) significantly enhanced to  $4.00 \pm 0.14$  MPa and  $2.10 \pm 0.35$  GPa,

respectively, after incorporation of DEX-LAP nanoplates (CPC-2) ( $P < 0.05$ ). It might be due to the inevitable impact of DEX-LAP nanoplates on the induction of higher nucleation sites and consequently extreme growth restriction of HA particles. However, after introducing 6% foaming agent (CPC-2-6), compressive strength and modulus declined to  $1.75 \pm 0.49$  MPa and  $0.90 \pm 0.13$  GPa, respectively. However, the obtained mechanical properties were still greater than those of pure non-porous CPC, showing the effective role of DEX-LAP nanoplates to control the mechanical properties of CPC. Moreover, compared to the mechanical properties of CPCs extracted from other research, the present results looked significant. For instance, in a research in which  $\text{Na}_2\text{HPO}_4$  and  $\text{NaH}_2\text{PO}_4$  were similarly used as liquid phases, the compressive strength of CPCs was reported approximately 1.3 MPa (DelReal *et al* 2002). In another research, Feng *et al* (2010) examined the impact of pore size and immersion time on the mechanical strength of CPC. They found that mechanical properties of CPCs reduced with increasing pore size. Noticeably, the CPC consisting of micropores with the



average size of 200–300  $\mu\text{m}$  revealed the compressive strength of 2.5–3 MPa. Montufar *et al* (2010) also designed a self-setting injectable hydroxyapatite scaffold to evaluate the impact of micropores on mechanical properties of CPC. They introduced micropores inside the structure of CPC by combining polysorbate 80 solution and liquid phase of CPC. They finally realized that the porous sample, with total porosity over 75%, revealed the weak mechanical strength (0.2 MPa). Therefore, we can conclude that while formation of uniform pores within CPC reduced the mechanical properties of CPC, DEX-LAP nanoparticles could positively control the mechanical properties of CPC.

### 3.2. *In vitro* drug release study

In order to promote osteoblast-like cell proliferation, DEX was incorporated into the LAP nanoplates. According to previous research, DEX could support the osteogenic differentiation of stem cells (Roozbahani *et al* 2017b). Therefore, in order to investigate the function of encapsulated DEX on the cellular behavior, the release of DEX from porous nanocomposite cements consisting of various amounts of foaming agents (CPC-2, CPC-2-3, and CPC-2-6) was investigated. Figure 6 established

that, the cumulative release amount of DEX meaningfully controlled by the porosity of the cement. DEX release profile from CPC-2 sample displayed three distinct stages consisting of an initial burst release, followed by a slight decrease in the DEX rate release and a constant release rate. Results showed that  $5.1 \pm 2.3\%$  release occurred in the first 3 h immersing of CPC-2 which was significantly less than that of in the previous reports (Loca *et al* 2015). The burst release is usual in the polymeric constructs owing to the aggregation of drug components on the membrane surface (Roy *et al* 2016). Herein, thanks to the consistent distribution of DEX molecules on the LAP nanoplates, less DEX exposed on the external of cement that delivered moderately fewer primary burst release. Even after formation of pores in the cement, the initial burst release did not considerably increase. Results showed that about  $10.1 \pm 1.2\%$  and  $19.7 \pm 1.2\%$  DEX released in the first 3 h immersing of CPC-2-3 and CPC-2-6, respectively. However, in contrary to the CPC-2 sample, the final stage of the DEX release did not reveal any constant release. Therefore, after 70 h of incubation, while the total amount of released DEX from CPC-2 were  $12.8 \pm 3.2\%$ , it was drastically boosted to  $54.1 \pm 3.4\%$  and  $70.0 \pm 3.3\%$  from CPC-2-3, CPC-2-6 samples, respectively. Forouzan-deh *et al* (2014) also evaluated the impact of

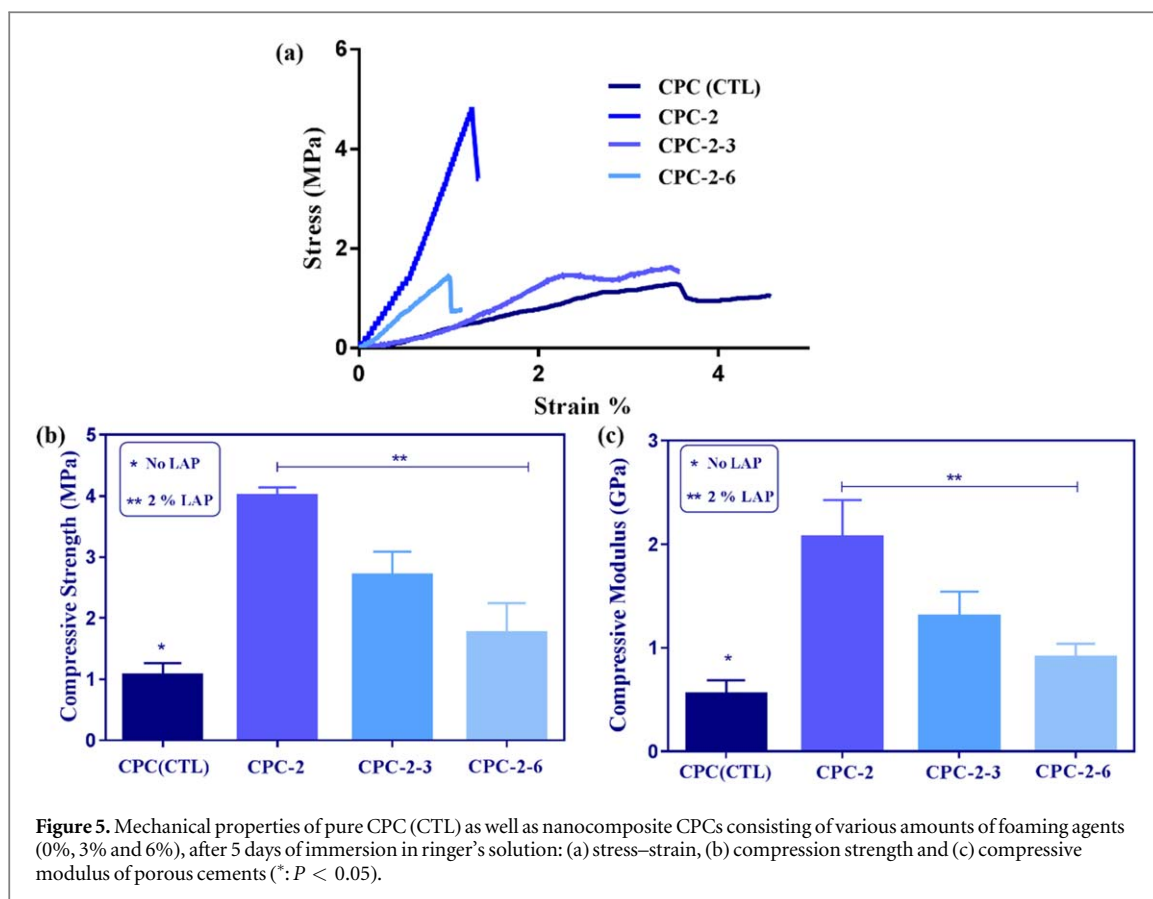


**Figure 5.** Mechanical properties of pure CPC (CTL) as well as nanocomposite CPCs consisting of various amounts of foaming agents (0%, 3% and 6%), after 5 days of immersion in Ringer's solution: (a) stress-strain, (b) compression strength and (c) compressive modulus of porous cements (\*:  $P < 0.05$ ).

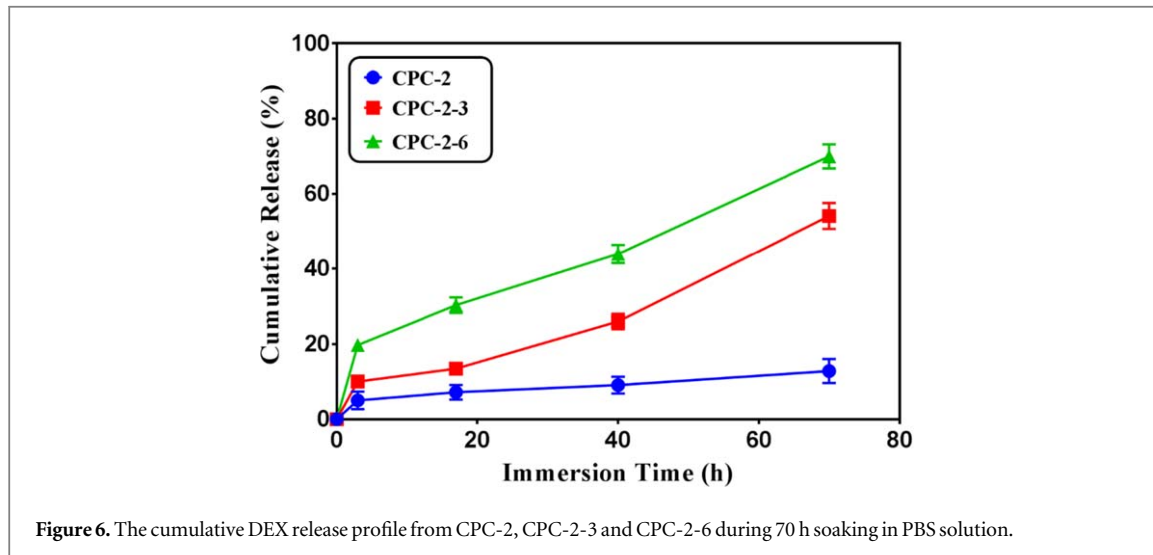


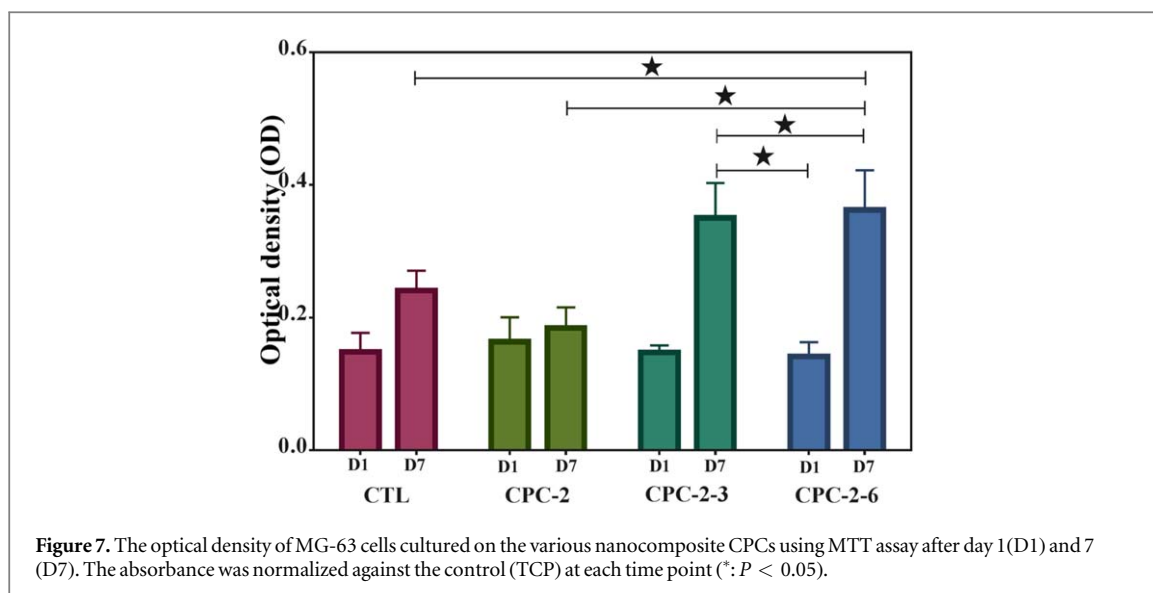
**Figure 6.** The cumulative DEX release profile from CPC-2, CPC-2-3 and CPC-2-6 during 70 h soaking in PBS solution.

micropore formation on the release rate of DEX from CPC. They found that while only 50% of the encapsulated DEX released from CPC, the presence of micropores resulted in the release of 90% DEX after 5 weeks could be due to the enhanced specific surface area leading to improve interaction between the aqueous solution and CPC and consequently fasten DEX release process. It could be suggested that superior pore size of the cement enhanced the penetration and diffusion of PBS through the cements facilitating DEX release from CPC matrix and subsequently enhanced the release rate.

However, considering our results, such a DEX release trend from whole nanocomposite cements could afford tolerable amounts of DEX supporting the promoted osteogenic differentiation of osteoblast-like cells.

### 3.3. Cell culture

In order to evaluate the effect of DEX-LAP nanoparticles as well as the amounts of pores on the viability of MG63 cells, MTT assay was carried out on cement samples upon 1 and 7 days of culture (figure 7). Generally, cell proliferation increased on the CPCs



and in the presence of DEX-LAP nanoparticles. For instance, the optical density of cells on the CPC-2 increased from  $0.16 \pm 0.04$  to  $0.18 \pm 0.03$  confirming that DEX-LAP nanoplates encouraged MG63 cell proliferation. Moreover, DEX release could be an efficient way to support cell proliferation. On the other hand, as foaming agent content went up in the structure of cement, the number of interconnected micropores created into the cement bulk enhanced, leading to the formation of suitable points for cells to penetrate, adhere, proliferate and grow. As clearly determined in figure 7, after 1 and 7 days of cell culture on CPC-2-6 sample, optical density of cells significantly increased from  $0.14 \pm 0.02$  to  $0.36 \pm 0.06$ . In another word, this porous cement revealed the higher cellular activity owing to possess deep and wide interconnected pores rather than other cement samples (CPC (CTL)). It was also noted that the presence of interconnected micropores could favor faster DEX delivery from LAP nanoplates which could promote cell viability. In general, the presence of both DEX-LAP nanoparticles, as a bioactive agent, and micropores, as suitable sites for cells to settle, in the structure of cement could promote survivability of cells making it a promising bone graft for filling bone defects.

#### 4. Conclusion

In this study, porous nanocomposite CPCs with fast setting and suitable mechanical characteristics were successfully developed via incorporation of DEX-LAP nanoplates. While the porous DEX-LAP/CPC possessed final setting time of  $9.6 \pm 1$  min, its compressive strength and modulus reached  $4.00 \pm 0.14$  MPa and  $2.10 \pm 0.35$  GPa, respectively. Moreover, sustained DEX release from LAP nanoplates was achieved led to enhanced MG63 cell proliferation, compared to CPC. Finally, porous DEX-LAP/CPC with promising properties may have applications in clinical situations

such as enhance bone screw fixation in osteoporotic bone that require fast setting, strong interfacial interaction with bone tissue and greater mechanical properties than commercial CPCs. In addition, porous DEX-LAP/CPC is easy to use without hand mixing using a dual syringe making it opportunity to use it as required throughout the operation. In addition, incorporation of DEX with anti-inflammation property in the bone cement may have the potential to significantly diminish inflammation in the joint replacements leading to reduced healing process.

#### ORCID iDs

Mahshid Kharaziha  <https://orcid.org/0000-0002-8803-105X>

#### References

- ASTM, C. 2003 *ASTM, Standard Test Methods for Time of Setting of Hydraulic Cement by Vicat Needle C191* (West Conshohocken, PA: ASTM International)
- Cama G and Barberis F 2009 Preparation and properties of macroporous brushite bone cements *Acta Biomater.* **5** 2161–8
- Carrow J K, Cross L M, Reese R W, Jaiswal M K, Gregory C A, Kaunas R and Gaharwar A K 2018 Widespread changes in transcriptome profile of human mesenchymal stem cells induced by two-dimensional nanosilicates *Proc. Natl Acad. Sci.* **115** E3905–13
- DelReal R P, Wolke J G C, Vallet-Regí M and Jansen J A 2002 A new method to produce macropores in calcium phosphate cements *Biomaterials* **23** 3673–80
- Del Valle S, Miño N, Muñoz F, González M, Planell J A and Ginebra M P 2007 *In vivo* evaluation of an injectable macroporous calcium phosphate cement *Mater. Sci.: Mater. Med.* **18** 353–61
- Feng B, Guolin M, Yuan Y, Changshen L, Zhen W and Jian L 2010 Role of macropore size in the mechanical properties and *in vitro* degradation of porous calcium phosphate cements *Mater. Lett.* **64** 2028–31
- Forouzandeh A, Hesaraki S and Zamanian A 2014 The releasing behavior and *in vitro* osteoinductive evaluations of dexamethasone-loaded porous calcium phosphate cements *Ceram. Int.* **40** 1081–91

- Fraile JM, Garcia-Martin E, Gil C, Mayoral JA, Pablo LE, Polo V and Vispe E 2016 Laponite as carrier for controlled *in vitro* delivery of dexamethasone in vitreous humor models *Eur. J. Pharm. Biopharm.* **108** 83–90
- Gaharwar A K, Cross L M, Peak C W, Gold K, Carrow J K, Brokesh A and Singh K A 2019 2D nanoclay for biomedical applications: regenerative medicine, therapeutic delivery, and additive manufacturing *Adv. Mater.* **31** 1900332
- Gaharwar A K, Kishore V, Rivera C, Bullock W, Wu C J, Akkus O and Schmidt G 2012 Physically crosslinked nanocomposites from silicate-crosslinked PEO: mechanical properties and osteogenic differentiation of human mesenchymal stem cells *Macromol. Biosci.* **12** 779–93
- Gaharwar A K, Mihaila S M, Swami A, Patel A, Sant S, Reis R L and Khademhosseini A 2013 Bioactive silicate nanoplatelets for osteogenic differentiation of human mesenchymal stem cells *Adv. Mater.* **25** 3329–36
- Gbureck U, Geffers M, Groll J and Gbureck U 2015 Dual-setting brushite–silica gel cements *Acta Biomater.* **11** 467–76
- Ghadiri M, Chrzanowski W and Rohanzadeh R 2015 Biomedical applications of cationic clay minerals *RSC Adv.* **5** 29467–81
- Ghadiri M, Hau H, Chrzanowski W, Agus H and Rohanzadeh R 2013 Laponite clay as a carrier for *in situ* delivery of tetracycline *RSC Adv.* **3** 20193–201
- Ginebra M-P, Canal C, Espanol M, Pastorino D and Montufar E B 2012 Calcium phosphate cements as drug delivery materials *Adv. Drug Deliv. Rev.* **64** 1090–110
- Ginebra M P, Driessens F C M and Planell J A 2004 Effect of the particle size on the micro and nanostructural features of a calcium phosphate cement: a kinetic analysis *Biomaterials* **25** 3453–62
- Ginebra M P and Montufar E B 2014 Injectable biomedical foams for bone regeneration *Biomed. Foams Tissue Eng. Appl.* **1** 281–312
- Ginebra M-P, Traykova T and Planell J 2006 Calcium phosphate cements as bone drug delivery systems: a review *J. Control. Release* **113** 102–10
- Hoppe A, Güldal N S and Boccaccini A R 2011 A review of the biological response to ionic dissolution products from bioactive glasses and glass–ceramics *Biomaterials* **32** 2757–74
- Kharaziha M, Fathi M H, Edris H, Nourbakhsh N, Talebi A and Salmanzadeh S 2015 PCL–forsterite nanocomposite fibrous membranes for controlled release of dexamethasone *J. Mater. Sci., Mater. Med.* **26** 1–11
- Kim S Y and Jeon S H 2012 Setting properties, mechanical strength and *in vivo* evaluation of calcium phosphate-based bone cements *J. Ind. Eng. Chem.* **18** 128–36
- Krüger R, Seitz J-M, Ewald A, Bach F-W and Groll J 2013 Strong and tough magnesium wire reinforced phosphate cement composites for load-bearing bone replacement *J. Mech. Behav. Biomed. Mater.* **20** 36–44
- Liu J, Li J, Ye J and He F 2016 Setting behavior, mechanical property and biocompatibility of anti-washout wollastonite/calcium phosphate composite cement *Ceram. Int.* **42** 13670–81
- Liu W, Zhai D, Huan Z, Wu C and Chang J 2015 Novel tricalcium silicate/magnesium phosphate composite bone cement having high compressive strength, *in vitro* bioactivity and cytocompatibility *Acta Biomater.* **21** 217–27
- Liu W, Zhang J, Rethore G, Khairoun K, Pilet P, Tancret F and Weiss P 2014 A novel injectable, cohesive and toughened Si-HPMC (silanized-hydroxypropyl methylcellulose) composite calcium phosphate cement for bone substitution *Acta Biomater.* **10** 3335–45
- Loca D, Sokolova M, Locs J, Smirnova A and Irbe Z 2015 Calcium phosphate bone cements for local vancomycin delivery *Mater. Sci. Eng. C* **49** 106–13
- Maenz S, Kunisch E, Mühlstädt M, Böhm A, Kopsch V, Bossert J and Jandt K D 2014 Enhanced mechanical properties of a novel, injectable, fiber-reinforced brushite cement *J. Mech. Behav. Biomed. Mater.* **39** 328–38
- Mohammadi M, Hesaraki S and Hafezi-Ardakani M 2014 Investigation of biocompatible nanosized materials for development of strong calcium phosphate bone cement: comparison of nano-titania, nano-silicon carbide and amorphous nano-silica *Ceram. Int.* **40** 8377–87
- Montufar E B, Traykova T, Gil C, Harr I, Almirall A, Aguirre A and Ginebra M P 2010 Foamed surfactant solution as a template for self-setting injectable hydroxyapatite scaffolds for bone regeneration *Acta Biomater.* **6** 876–85
- Müller F A, Gbureck U, Kasuga T, Mizutani Y, Barralet J E and Lohbauer U 2007 Whisker-reinforced calcium phosphate cements *J. Am. Ceram. Soc.* **90** 3694–7
- Park J K, Choy Y B, Oh J-M, Kim J Y, Hwang S-J and Choy J-H 2008 Controlled release of donepezil intercalated in smectite clays *Int. J. Pharm.* **359** 198–204
- Perut F, Montufar E B, Ciapetti G, Santin M, Salvage J, Traykova T and Baldini N 2011 Novel soybean/gelatine-based bioactive and injectable hydroxyapatite foam: material properties and cell response *Acta Biomater.* **7** 1780–7
- Roozbahani M, Alehosseini M, Kharaziha M and Emadi R 2017a Nano-calcium phosphate bone cement based on Si-stabilized  $\alpha$ -tricalcium phosphate with improved mechanical properties *Mater. Sci. Eng. C* **81** (Suppl. C) 532–41
- Roozbahani M, Kharaziha M and Emadi R 2017b pH sensitive dexamethasone encapsulated Laponite nanoplatelets: release mechanism and cytotoxicity *Int. J. Pharm.* **518** 312–9
- Roy A, Jhunjhunwala S, Bayer E, Fedorchak M, Little S R and Kumta P N 2016 Porous calcium phosphate-poly (lactic-co-glycolic) acid composite bone cement: a viable tunable drug delivery system *Mater. Sci. Eng. C* **59** 92–101
- Ruzicka B and Zaccarelli E 2011 A fresh look at the Laponite phase diagram *Soft Matter* **7** 1268–86
- Shahrezaei M, Shahrouzi J, Hesaraki S and Zamanian A 2014 The effect of  $\alpha$ -TCP particle size on mechanical and setting properties of calcium phosphate bone cements *J. Arch. Mil. Med.* **2** e16516
- Takagi S and Chow L C 2002 Formation of macropores in calcium phosphate cement implants *Mater. Sci.: Mater. Med.* **12** 135–9
- Tancret F and Liu W 2014 A novel injectable, cohesive and toughened Si-HPMC (silanized-hydroxypropyl methyl cellulose) composite calcium phosphate cement for bone substitution *Acta Biomater.* **10** 3335–45
- Tang M, Weir M D and Xu. H H 2012 Mannitol-containing macroporous calcium phosphate cement encapsulating human umbilical cord stem cells *Tissue Eng. Regen. Med.* **6** 214–24
- Verron E, Boulter J M and Guicheux J 2012 Controlling the biological function of calcium phosphate bone substitutes with drugs *Acta Biomater.* **8** 3541–51
- Wang C, Wang S, Li K, Ju Y, Li J, Zhang Y and Zhao Q 2014 Preparation of Laponite bioceramics for potential bone tissue engineering applications *PLoS One* **9** e99585
- Wang S, Wu Y, Guo R, Huang Y, Wen S, Shen M and Shi X 2013 Laponite nanodisks as an efficient platform for doxorubicin delivery to cancer cells *Langmuir* **29** 5030–6
- Xu H H and Quinn J B 2002 Calcium phosphate cement containing resorbable fibers for short-term reinforcement and macroporosity *Biomaterials* **23** 193–202
- Xu H H, Weir M D and Simon C G 2008 Injectable and strong nanoparticle scaffolds for cell/growth factor delivery and bone regeneration *Dent. Mater.* **24** 1212–22
- Xue Z, Zhang H, Jin A, Ye J, Ren L, Ao J and Lan X 2012 Correlation between degradation and compressive strength of an injectable macroporous calcium phosphate cement *J. Alloys Compd.* **520** 220–5
- Zhao P, Zhao S, Zhao T R, Ren X H, Wang F and Chen X N 2012 Hydroxyapatite whisker effect on strength of calcium phosphate bone cement *Adv. Mater. Res.* **534** 30–3